NASA Radar Altimeter for the TOPEX/POSEIDON Project

ALFRED R. ZIEGER, DAVID W. HANCOCK, GEORGE S. HAYNE, MEMBER, IEEE, AND CRAIG L. PURDY

Invited Paper

Over-ocean radar altimetry combines precision orbit determination (POD) and precise measurements from the sea surface to the satellite center-of-mass to infer the topography of the ocean surface under study. The radar altimeter provides one element of this measurement, i.e., the distance from the sea surface to the satellite. The NASA Radar Altimeter (NRA) is a fifth generation U.S. altimeter that will provide the primary measurement for the TOPEX/POSEIDON Project altimetric mission. We present the requirements, altimeter fundamentals, design description, integration and test program, primary elements of ground processing, and assessment for the dual frequency NASA Radar Altimeter.

I. Introduction

The TOPEX/POSEIDON Project is a joint U.S. and French mission to develop and operate an Earth-orbiting satellite with sensors capable of making accurate measurements of sea level. The primary measurement is made by radar altimetry, and the proof-of-concept of this was demonstrated by the Seasat Mission in 1978 [1], [2] and the Geosat Mission in 1985 [3], [4]. The mission objective is to measure the sea level in a way that allows the study of ocean dynamics, including the calculation of the mean and variable surface geostrophic currents and the tides of the world's oceans. This will aid in understanding global ocean dynamics, climatology, and meteorology. Figure 1 depicts the instrument development and mission operations schedule. The NRA is the first dual frequency altimeter. It operates at 5.3 GHz and 13.6 GHz, C- and Ku-band, respectively. The dual frequency design allows for height measurement corrections due to the ionospheric effects on the signal.

Manuscript received December 17, 1990; revised February 15, 1991. The altimeter work described was carried out by the Jet Propulsion Laboratory, California Institute of Technology, Goddard Space Flight Center, and Johns Hopkins University/Applied Physics Laboratory as part of the TOPEX/POSEIDON Project under contract with NASA.

A.R. Zieger is with the Jet Propulsion Laboratory, Pasadena, CA 91109.

D.W. Hancock, G.S. Hayne, and C.L. Purdy are with the Goddard Space Flight Center, Wallops Island, VA 23337.

IEEE Log Number 9100193.

The TOPEX/POSEIDON satellite, provided by Fairchild Space, will host the NRA and other scientific instruments. Good satellite/antenna pointing minimizes the error in off-nadir pointing corrections. The NRA will measure the local height to a precision of about 2 cm over a 3 s average of data. The satellite configuration with instrumentation is shown in Fig. 2.

The primary goal of the TOPEX/POSEIDON Mission is to substantially increase our understanding of the global ocean dynamics. This is done by making precise and accurate observations of the oceanic topography for several years. These measurements will contribute toward the determination of the general circulation of the ocean and its variability. This will permit studies of the role of the oceans in the earth's climate system, how much carbon dioxide enters the oceans, calculation of the transport of heat by the oceans, and tests of the ability to compute circulation from the forcing by winds.

The sensors payload has several improvements over previous missions. The altimeter design was upgraded to a dual frequency instrument to provide a path delay correction for ionospheric effects in the radar beam. The altimeter antenna diameter was increased to 1.5 m from the 1.0 m antenna used on Seasat/Geosat. The larger antenna retains a strong signal-to-noise ratio at the higher TOPEX/POSEIDON mission altitude. The precision orbit is determined and maintained more easily at the higher altitude where atmosphere drag is greatly reduced. The Ku-band pulse repetition frequency (PRF) was increased by approximately a factor of four to provide improved precision at higher ocean wave heights. The microwave radiometer has fixed pointing in the nadir direction which provides an increased integration interval in the vertical. Both Seasat and Nimbus radiometers were forward looking scanning instruments. Also, the radiometer multifrequency feed horn was modified to improve beam efficiency at the 18, 21, and 37 GHz frequencies being used to provide

0018-9219/91/0600-0810$01.00 © 1991 IEEE

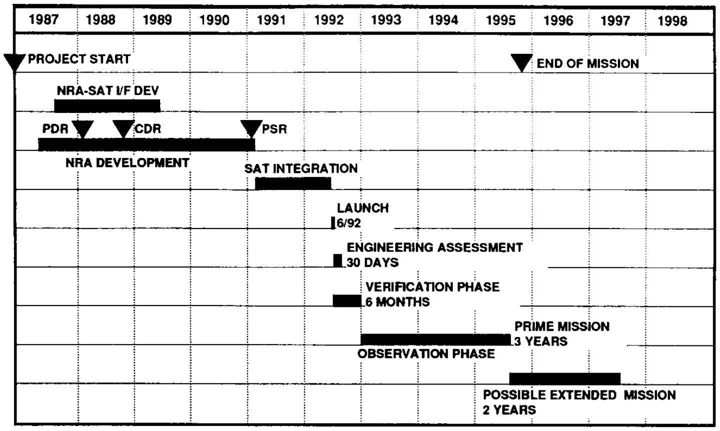

Fig. 1. Instrument development, integration, test, and mission operations.

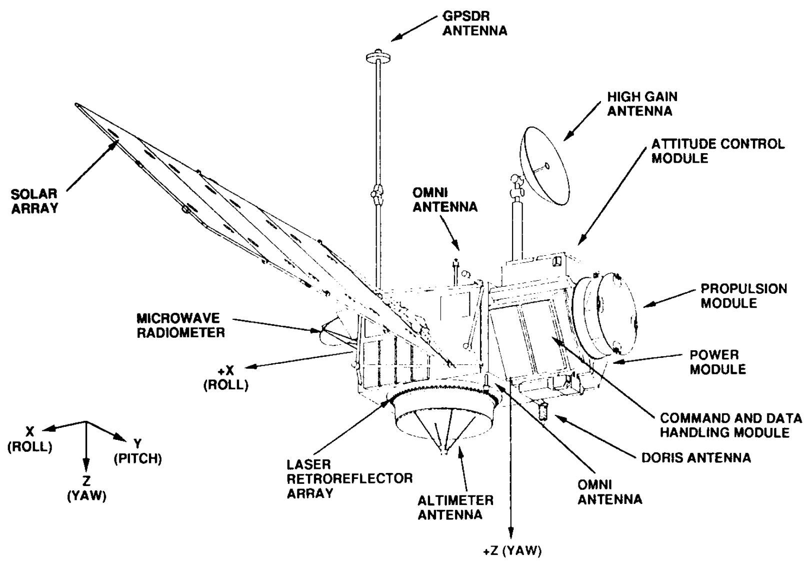

Fig. 2. Satellite configuration with instrumentation.

measurements to make the wet troposphere path delay correction.

The joint oceanographic project is managed by the Jet Propulsion Laboratory/California Institute of Technology (JPL/CIT) on NASA's behalf. NASA and the Centre National d'Etudes Spatiales (CNES) share in the joint cooperative space project. The NRA is the primary instrument within the TOPEX/POSEIDON Sensors System. The Goddard Space Flight Center (GSFC) is the organizational element of the project responsible for developing the NRA. In particular, the GSFC Wallops Flight Facility (WFF) is managing the altimeter procurement which was given to the Johns Hopkins University/Applied Physics Laboratory (JHU/APL). A second experimental altimeter is being provided by CNES. The CNES Altimeter is a single channel Ku-band (13.65 GHz) solid-state amplifier device, designed for low mass, and low power. This first generation altimeter is planned to be flown on future French missions. A common 1.5 m parabolic antenna is shared by the NASA and CNES altimeters. The altimeters share the antenna through an orthomode coupler at the base of the multifrequency feed horn. This paper concentrates on the description of the NRA.

The launch of the TOPEX/POSEIDON satellite in June/July of 1992 will begin the in-flight operation of the joint NASA/CNES project. The satellite will be launched by an Ariane 42P launcher from Kourou, French Guiana. The nominal operational orbit is nearly circular, with an altitude of 1334 km, an inclination of 66 degrees and an orbital period of 112 minutes. The orbit repeats its ground traces every 127 revolutions (about 10 days). The geographical repetition of the ground traces allows for the observation of variability in the sea surface topography.

II. Principal Altimeter Requirements

The NRA is a dual-frequency design that operates at C-band (5.3 GHz) and Ku-band (13.6 GHz) frequencies. These frequencies were selected because they provide adequate signal penetration of the troposphere and they are within the permissible frequency bands established by international committees. The orbital parameters for the NRA range of operation shall be within:

11) altitude = 1334 ± 60 km;

12) inclination = 62 to 67 degrees;

13) eccentricity = < 0.001.

Additional requirements for altimeter velocity, acceleration, power, pointing, and the radiation environment are derived from the above orbital conditions. The constraints under which the performance requirements shall be met are as follows [5]:

- Ku-band and C-band bandwidth of 320 MHz, with C-band selectable at 100 MHz;
- antenna control pointing accuracy of 0.14 degree (1-sigma);
- 2-m significant wave height ($H_{1/3}$);
- wave distribution skewness ≤ 0.1;
- rain rate ≤ 2.0 mm/h;

The specific altimeter performance requirements are listed as follows [5]:

1) Provide an output of height measurements averaged over 1-s and 3-s intervals so that, after correction for ionospheric delay and independent of geographical location, 68% of the data points have the precision indicated below:

1-Second	3-Second
(a) ≤ 4.2 cm for 2-m $H_{1/3}$	≤ 2.4 cm for 2-m $H_{1/3}$
(b) ≤ 4.7 cm for 4-m $H_{1/3}$	≤ 2.7 cm for 4-m H_{1/3}
(c) ≤ 5.5 cm for 8-m $H_{1/3}$	≤ 3.2 cm for 8-m $H_{1/3}$

2) Provide track acquisition within 5 s of losing lock in either dual channel (Ku- and C-band) or single channel (Ku- or C-band) operation.

3) Determine the altitude rate within 1 cm/s over a ±50 m/s rate.

4) Provide the capability for operation over the acceleration range of ± 1 m/s^2.

5) Design for a 3 year lifetime and the option for a 2 year extended mission.

6) Provide the capability for a maximum detectable height drift of ≤ 2 cm per 10-day period after appropriate calibrations.

7) Relative time tagging shall be within ±10 μs of spacecraft time at the altimeter spacecraft interface.

8) Develop an interface with the CNES Radar Altimeter that provides at least 30 dB of isolation between the radar signals from the two altimeters.

9) Provide waveform data sets for each channel that will allow assessment and evaluation of altimeter performance.

10) Physical design allocations are for a power of 238 W, mass of 214 kg, and an antenna diameter of 1.5 m. These limits afford compatibility with the spacecraft design.

11) The combined channel telemetry rate shall not exceed 10 kb/s average data rate.

III. NASA Radar Altimeter Conceptual Design

The NRA instrument described as follows is a pulse radar designed to measure to high accuracy the time from transmitted signal to received echo from the ocean surface, thereby determining the range from satellite orbit to surface. The altimeter range measurement and corrections are shown schematically in Fig. 3. Since the orbit shape is determined independently, a measure of the shape of the ocean surface can be found. In absence of dynamic oceanographic features such as tides and currents, the shape of the surface will conform to the gravitational equipotential surface, the geoid. If the geoid is adequately known, the altimeter measurements will allow estimation of the dynamic oceanographic effects causing the ocean surface to depart from the geoid. The altimeter also determines the slope of the return waveform's leading edge, and the return power level. The waveform leading edge slope produces an estimate of the ocean's significant waveheight (SWH), and the return power level produces an estimate of the ocean surface's radar backscatter cross-section σ°. Based on earlier correlation of radar altimeter σ° with ocean surface wind speed, the σ° can provide ocean wind speed estimates but not direction [6], [7].

Descriptions of radar altimeters are available for Skylab S-193 [8], Geos-3 [9], Seasat [10], [11], Geosat [12], and the TOPEX NRA [13], [14]; see also [15]. The several journal special issues devoted to satellite altimetry include results from Geos-3 [16], Seasat [1], [2], [17], and Geosat [3], [4].

A. Basic Altimeter Review and NRA Details

The basic altimeter operation principle can be found in [18]. We only give a brief tutorial here for completeness. We begin by describing the interaction of a short radar pulse with a planar, incoherently scattering surface and then describe the modification necessary for the finite curvature of the Earth's surface. The general radar altimeter return waveform model is then summarized. Next the specific TOPEX NRA waveform sampling gates and operation of the range tracker are described. The altimeter range estimate has an error which is a function of SWH and attitude angle, and correction for this error is also described.

Suppose at time $T = 0$, a radar pulse of infinitesimal time duration is emitted by a radar transmitter a height H above an incoherently scattering planar surface. Assume that the scattering elements are densely and uniformly

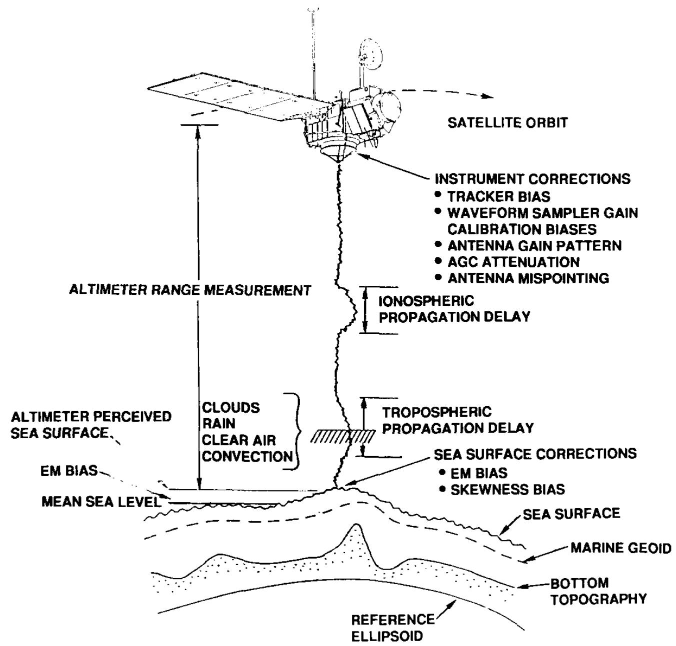

Fig. 3. The altimeter range measurement and corrections are illustrated schematically to show the geometry of the measurement.

distributed over the plane. For any time $T > 0$, the locus of points from which the receiver could have received scattered energy returned from the pulse is a spherical shell (of infinitesimal thickness) of radius $cT/2$ about the radar altimeter position;[2] whether the receiver actually does receive a return at time $T > 0$ depends on whether any surface scattering element is intercepted by the spherical shell. There will be no received energy at any time T such that$cT/2 < H$, or $T < 2H/c$. At the time $T = 2H/c$, the receiver will see the first return from the nadir point, the point on the plane surface closest to the altimeter. At any time $T > 2H/c$, the received energy will come from points on the circumference of a circle about the nadir point on the surface, the circle which is the intersection of the spherical shell with the plane surface.

Now replace the infinitesimal pulse at $T = 0$ by an idealized rectangular pulse of width τ_p which starts at $T = -\tau_p/2$ and stops at $T = +\tau_p/2$. The power received from the transmitted pulse of duration τ_p centered at T = 0 will be zero for all $t < -\tau_p/2$, will increase linearly with t from $t = -\tau_p/2$ to $t = +\tau_p/2$, and will be constant for all $t > +\tau_p/2$. The maximum uniformly illuminated circle seen by the altimeter will have the radius r_τ given by

$$r\tau = (Hc\tau_p)^{1/2} \tag{1}$$

[2] The factor $c/2$ appears because round-trip time is being considered, the time the energy is received back at the receiver, not the time that energy first reaches the surface.

(at time $t = +\tau_p/2$) and thereafter the illuminated area seen will be an annulus. The quantity r_τ is referred to as the footprint radius for the pulse-limited radar altimeter. The return radar power thus will have three separate regions: i) baseline (before any surface illumination); ii) leading-edge, with power increasing linearly with time (as the illuminated circle grows from 0 to r_τ); and plateau (when the surface illuminated is an annulus). This principle is illustrated in Fig. 4.

Figure 5 presents a linear-FM transmitted pulse, which varies by 320 MHz over a time 102.4 μs. The pulse is scattered from separate elements 1, 2, and 3 on the ocean surface, these correspond respectively to the crest, slope, and trough of a wave. The return signals are mixed with a local oscillator (LO) signal which is a properly timed replica of the chirp pulse, with the result that signals from the three different surface heights are transformed into three separate frequencies at the output of the mixer. Then by Fourier analysis techniques the return signal can be separated into a number of discrete frequency samples.

Moore and Williams [19] demonstrated that the average radar power return from a rough surface for near-normal incidence scattering could be expressed as a convolution of: 1) the transmitted pulse shape and 2) a term which included effects of antenna pattern, off-nadir pointing angle, surface properties, and distance. Brown [20] used this convolutional model with assumptions common to satellite radar altimeter systems to produce a simplified closed-form expression for the average rough surface impulse response function, and

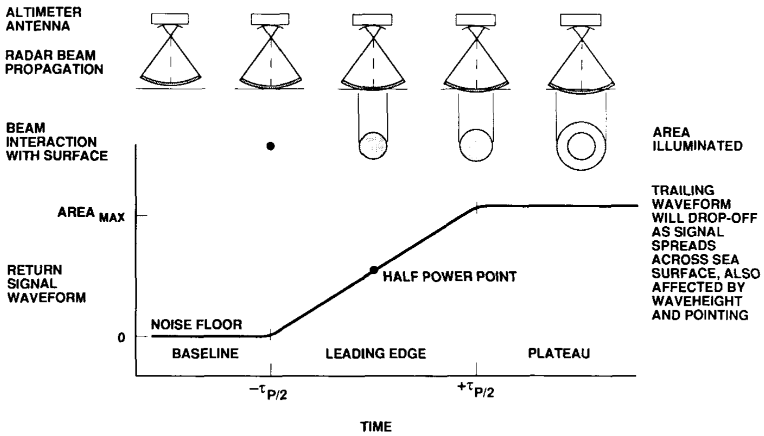

Fig. 4. Altimeter pulse interaction with the sea surface and the characteristic return waveform generated by the altimeter electronics.

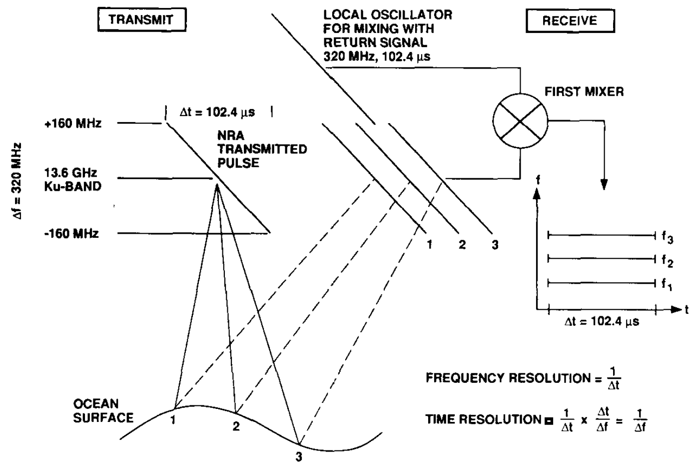

Fig. 5. Linear FM transmitted pulse, varying by 320 MHz over a time of 102.4 μs. The pulse is scattered from separate elements 1, 2, and 3 on the ocean surface.

Rodriguez [21] pointed out the importance of correcting the Brown flat-surface results by the factor $(1 + H/R_e)$ to account for the finite radius of the earth. In this approach, the altimeter mean return waveform $W(t)$ is given by the convolution of three terms,

$$W(t) = P_{FS}(t) * q_s(t) * p_\tau(t) \ , \tag{2}$$

where $P_{FS}(t)$ is the flat-sea impulse response function including radar antenna beamwidth and pointing angle effects, $q_s(t)$ is the radar-observed surface elevation probability density function, and $p_\gamma(t)$ is the radar altimeter's point-target response function.

The flat-sea impulse response function is given by

$$P_{FS}(t) = A_0 \exp(-\delta t) I_0(\beta t^{\frac{1}{2}}) U(t) \tag{3}$$

in which

$$\delta = (4/\gamma)\ (c/H)\ (1 + H/R_e)^{-1} \cos(2\xi) \tag{4}$$

and

$$\beta = (4/\gamma)\ (c/H)^{\frac{1}{2}}\ (1 + H/R_e)^{-\frac{1}{2}} \sin(2\xi) \tag{5}$$

where $U(t)$ is a unit step function, and $I_0(\beta t^{\frac{1}{2}})$ is a modified Bessel function. H is the spacecraft height above the surface, R_e is the earth's radius, c is the speed of light, ξ is the absolute off-nadir pointing angle (or attitude angle), and γ is an antenna beamwidth parameter defined by assuming a Gaussian approximation to the antenna gain for an angle θ off the antenna's axis,

$$G(\theta) = G_0 \exp[-(2/\gamma) \sin^2 \theta] \ . \tag{6}$$

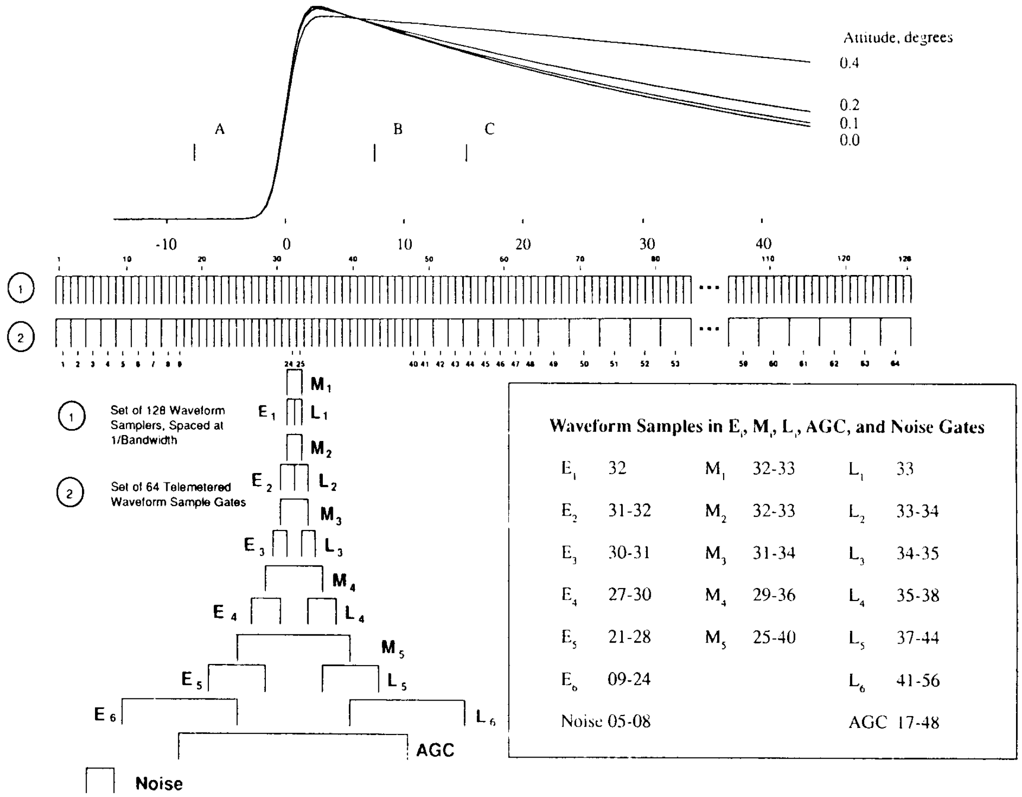

Waveform Samples in E, M, L, AGC, and Noise Gates

E_1	32	M_1	32-33	L_1	33
E_2	31-32	M_2	32-33	L_2	33-34
E_3	30-31	M_3	31-34	L_3	34-35
E_4	27-30	M_4	29-36	L_4	35-38
E_5	21-28	M_5	25-40	L_5	37-44
E_6	09-24			L_6	41-56
Noise	05-08			AGC	17-48

Fig. 6. Ku-band mean waveform telemetered to ground by 128 samplers grouped by selective gates. A gate is the arithmetic average of a specified number of waveform samplers.

If θ_w is the usual antenna angular full-width at half-power, then

$$4/\gamma = (\ln 4)/\sin^2(\theta_w/2)\ . \tag{7}$$

The amplitude term A_0 includes several other constants:

$$A_0 = \{[G_0 \lambda_r^2 c \sigma^\circ(0)]/[4(4\pi)^2 L_p H^3 (1 + H/R_e)^3]\} \cdot \exp[-(4/\gamma)\sin^2 \xi \tag{8}$$

where

λ_r radar wavelength,
$\sigma^\circ(0)$ ocean's radar backscattering cross-section at normal incidence,
G_0 radar antenna's boresight gain,
L_p two-way propagation path loss.

In the NRA, the radar return signals are normalized by the automatic gain control (AGC) circuit, and we can ignore all individual scaling terms within the A_0 above, Instead A_0 is treated as a simple amplitude scaling term which is adjusted in any fitting of waveform sample data to the general model $W(t)$.

The radar-observed ocean surface elevation probability distribution function $q_s(t)$ is assumed to be the skewed Gaussian form given in the time domain by

$$q_s(t) = [(2\pi)^{\frac{1}{2}} \sigma_s]^{-1} \{1 + (\lambda_s/6)[(t/\sigma_s)^3 - 3(t/\sigma_s)]\} \cdot \exp[-(t/\sigma_s)^2/2] \tag{9}$$

where σ_s is the surface rms elevation in ranging-time units, and λ_s is the surface skewness parameter.

The point-target response $p_\gamma(t)$ is the effective transmitted pulse shape as observed by the receiver, and it has a theoretical shape of $(\sin^2 x)/x^2$. When fitting actual radar altimeter data, the sampled data from one of the altimeter's calibration modes is used for the actual $p_\gamma(t)$. Based on these functional formula, the parameters of the ocean were estimated by fitting waveform sampler data to the model waveform.

Often the model waveform fitting is done by an iterative procedure [22] which systematically varies the waveform model parameters to achieve a best fit in a least squares sense. There are other investigations which use deconvolution methods [23].

B. NRA On-Board Gate Selection and Range-Tracking

The NRA has a set of 128 waveform samplers, uniformly spaced with 3.125 ns separation. Figure 6 shows the portion of the TOPEX Ku-band mean waveform which will be sampled by these 128 samplers; the curves are for a case where the SWH of the ocean is 4 m, with different attitude angles from 0.0 to 0.4 degrees. The horizontal scale is labeled in range relative to the nominal track point on the leading edge of this waveform. The E, M, and L designate Early, Middle, and Late Gates, respectively. Notice also the AGC Gate and the Noise Gate. Table 1 summarizes the way in which the 128 waveform samples will be averaged to form the 64 telemetry samples. The telemetry samples are averages of either two or four update intervals, either 10 or 5 per second; usually the higher rate samples will come from the Ku-band altimeter and the lower rate from the C-band altimeter, but these data rates can be reversed by command.

As in the earlier Seasat instrument [11], the TOPEX instrument positions the track-point so that $(S*AGC - M_i)$ is zero, where S is a near-unity scaling factor. In Seasat, S was 60/53; for TOPEX, the Ku-band S and the C-band S will also be near unity, the final values will be selected after testing. There are five different possible M_i, and the choice is made based on the SWH; for higher SWH it is desirable to use a wider Middle Gate. A significant waveheight-related quantity V_{SWH} is defined, for i of 1 through 5, by

$$V_{SWH,i} = (L_i - E_i)/(L_6 - E_6) \, . \tag{11}$$

Figure 7 shows all five TOPEX Ku-band $V_{SWH,i}$ values plotted versus SWH, for an attitude angle of 0.1 degrees. The TOPEX tracker logic requires choice of i such that the $V_{SWH,i}$ lies closest to a reference value, 0.64 in this figure. The heavy-line portions of the five V_{SWH} in this figure indicate which i is chosen for any given SWH. The telemetry stream contains i, designated the gate-selection index, and the $V_{SWH,i}$ for that i.[3] The gate-selection index chosen by this SWH-related logic then selects which of the M_i to use in the tracking algorithm.

For small deviations around the range track-point, the quantity $(S*AGC - M_i)$ is proportional to the range error. This range error updates the second-order $\alpha - \beta$ range-tracking loop at an approximately 20-Hz rate, and the range and range rate estimates are both put in the telemetry stream at the track update rate.

C. Ionospheric Propagation Delay and Its Correction

The radar signal speed in the ionosphere is changed by an amount proportional to the total columnar electron content along the propagation path. The electron content is expressed in units of TEC, where a TEC of 1 equals 10^{16} electrons per square meter. In a review of propagation path effects in high precision satellite altimetry [24], it is shown that the range correction for total ionospheric electronic content is

$$\Delta h = 40.3 TEC/f^2 \tag{12}$$

where Δh is in centimeters, and the radar frequency f is in GHz. If two range measurements are made, range H_L at a lower frequency f_L and range H_U at an upper frequency f_U, the true or unmodified range H_T can be shown to be

$$H_T = (K \cdot H_U - H_L)/(K - 1) \tag{13}$$

where

$$K = (f_U/f_L)^2 \, . \tag{14}$$

The range noise of the corrected (or true) range, σ_T is, in terms of the range noise σ_U and σ_L, given by

$$\sigma_T = [K/(K-1)] \cdot [\sigma_U^2 + (\sigma_L/K)^2]^{\frac{1}{2}} \, . \tag{15}$$

[3] In Seasat and Geosat, the SWH estimate was produced in an on-board table look-up procedure. TOPEX will do the equivalent of the table look-up in the ground processing. One of the advantages of having the V_{SWH} in the telemetry stream is increased resolution on the final SWH. Also for ground-based corrections to the on-board tracker's range estimate for effects of SWH and attitude angle, the V_{SWH} is a more natural parameter to use than the derived SWH.

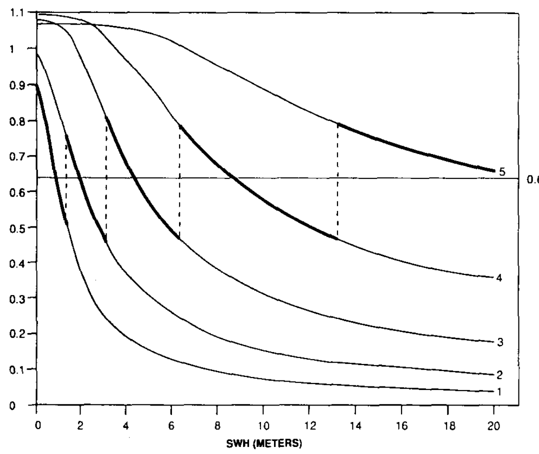

Fig. 7. Significant waveheight-related quantity, V_{SWH}, shown for Ku-band values plotted versus SWH for a 0.1 degree attitude angle.

Table 1 Relationship of Waveform and Telemetry Samples

Waveform Sample Number (set of 128)	Telemetry Sample Number (set of 64)
1, 2	1
3, 4	2
...	...
15, 16	8
17	9
18	10
...	...
48	40
49, 50	41
51, 52	42
...	...
63, 64	48
65, 66, 67, 68	49
69, 70, 71, 72	50
...	...
121, 122, 123, 124	64

Table 2 NASA Radar Altimeter Characteristics

Item	Parameter	Description
Transmitted Waveform	Chirp modulation	Linear FM sweep
	Center frequency	13.6 GHz (main) 5.30 GHz (Iono.)
	Pulse width (PW)	102.4 μs
	Bandwidth (BW)	320 MHz
	C Selectable PW/BW	32 μs/100 MHz
	Pulse period	204.8 μs
	Burst period (1334 km)	8893 μs
	Pulse repetition frequency	4200 (Ku) 1220 (C)
Antenna	Type	1.5-m parabola
	Gain	43.9 dB (Ku), 35.7 dB (C)
	Beamwidth	1.1 deg (Ku) 2.7 deg (C)
Transmitter	Peak power	20 W (Ku) 20 W (C)
	Duty factor	46% (Ku) 12% max. (C)
	Power Consumption	70 W (Ku) 28 W (C)
Signal Processor	Waveform samples	128 per channel
	Range resolution	0.5 m
	Tracker type	Alpha-Beta
Operation Modes	Idle	While CNES Altimeter ON
	Standby	Not transmitting
	Track	4 track modes
	Calibrate	4 calibrate modes
	Test	4 test modes
Inputs	Power bus	23-35 V dc
	Timing signal	5 MHz (0.8 V p-p)
	Commands	Relay (20, 1/s) Data (16-b, 1 kb/s)
Outputs	Telemetry	1228 byte frame
	Rate	About 9.8 kb/s
Power Demand	Idle	141 W
	Standby	226 W
	Calibrate, test	226 W
	Track	232 W
Weight	Complete unit	219 kg

IV. NRA Sensor Design

The radar altimeter design, as described in Table 2, is based on the Seasat and Geosat altimeters. However, its design incorporates several changes from those altimeters to provide for a more precise height measurement, better accuracy, and a longer operational lifetime. The functional design of the NRA is provided in Fig. 8. The Ku-band PRF will be approximately 4200 pulses per second and the C-band will be approximately 1220 pulses per second. The higher PRF provides for better height precision for ocean waveheights up to 20 m. The pulses will be transmitted in a fixed burst (38 Ku-band and 10 C-band per burst) with a variable spacing between bursts that is adjusted by the height measurement. The burst mode interleaving of signals is shown in Fig. 9. This dual frequency operation also requires a dual frequency antenna (described as follows). A new tracking/acquisition algorithm is used which will allow for more and better quality data at land/sea interfaces. Four steps are included: 1) coarse acquisition, 2) coarse track, 3) fine acquisition, and 4) fine tracking. This should allow the altimeter to logically step back when tracking becomes difficult to some point other than complete reacquisition. As the altimeter does step back, data of increasingly worse precision will be available; but the data will be much better than if the full reacquisition cycle had to be executed. This mode does not require a CW transmission for acquisition as have previous altimeters. To meet the project-required lifetime of 3 years (goal of 5 years) the altimeter has been designed to have fully redundant sides except for the antenna and some of the passive components in the microwave front end (transmit and receive portions). Cross-strapping of individual units had been considered, earlier in the project, but it was found that no increased reliability benefit was realized when proper account of the varying types and complexity of the unit-to-unit interfaces was included in the reliability calculations.

The redundant "sides" of the altimeter are designed for completely independent operation from each other. All interfaces for each side of the altimeter with the spacecraft are independent and cross-strapped where possible. Only one side of the redundant altimeter is operated at a time. Emergency uplink reprogramming is also included. This capability allows modification inflight of any portion or all of the system flight software. A parameter select mode will also be included which will allow changing many of the altimeter operating parameters (time constants, threshold values, etc.). This mode does not require full reprogramming but rather a parameter select upload.

The NRA comprises 22 individual subsystems (boxes) and an antenna. These subsystems are integrated and mounted in the nadir portion of the satellite instrument module (provided by the spacecraft contractor). This nadir portion is called the F-section. Figure 10 shows an isometric drawing of the F-section and the altimeter subsystems mounted as they will be for flight. Figure 11 is a photograph of the altimeter hardware located internally in the instrument module. The electronics boxes are mounted internal to the instrument module and the antenna is mounted externally on the nadir-facing panel.

The overall block diagram shows the full system redundancy and the interface to the spacecraft systems. All systems (except the antenna), and both microwave transmission units (MTU) are fully redundant; the active circuitry (amplifiers, switch drivers, etc.) within each MTU is fully redundant for each frequency. The redundant altimeters use the nomenclature of "Side A" and "Side B." The altimeter side for operation can be chosen via a series of ground issued commands. In describing the design, only one side of the altimeter will be considered.

Functionally, the altimeter can be considered to be a RF section comprising those units in column A of Table 3, a digital section comprising those units in column B of the

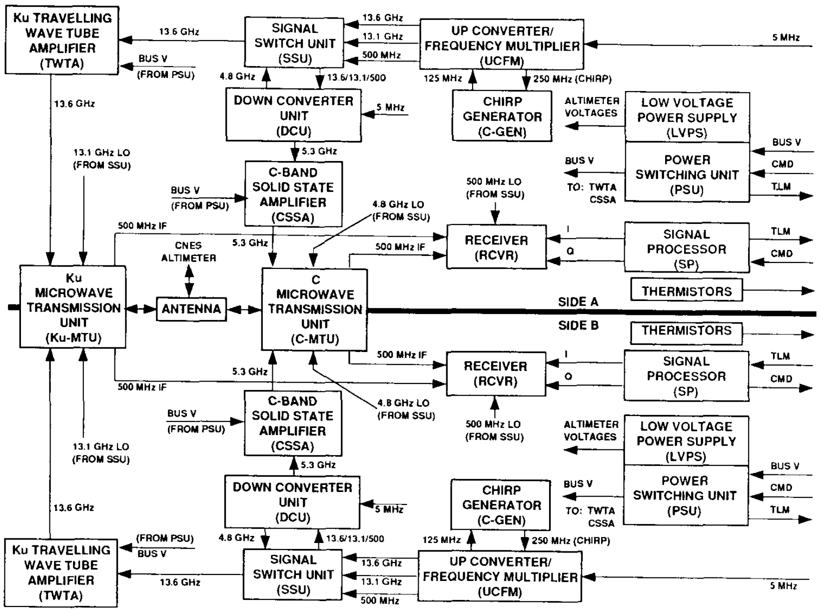

Fig. 8. The functional block diagram of the NRA illustrates the side A and side B redundancy concept used to attain a 3 year design life of 0.9 probability.

table, a power supply (consisting of the low voltage power supply and the power switching unit), and a dual-frequency antenna.

The up converter frequency multiplier (UCFM) receives a stable 5-MHz clock signal from the spacecraft and produces higher frequency signals for use elsewhere in the altimeter. It generates a 125-MHz signal for use in the chirp generator unit.

The chirp generator then returns a 250-MHz chirped (frequency modulated) signal with the desired bandwidth based on the mode of operation (nominally 80 MHz). From this the UCFM produces a 13.6 GHz chirped signal for the Ku-band transmission and a 13.1 GHz chirped signal for the Ku-band LO. The chirp bandwidths of these signals are identical, 320 MHz for the normal track mode. The pulsewidth of each signal is 102.4 μs. The UCFM generates a 500 MHz CW signal for the second downconversion process in the receiver unit. The UCFM also generates an 80 MHz CW clock signal for use in the digital signal processor unit.

The chirp generator comprises a digital section and a RF section. The digital section under external control generates inphase (I) and quadrature (Q) signals for use in the RF section. These I&Q signals determine the signal bandwidth and the chirp slope. The RF section modulates the 125 MHz signal from the UCFM with the I&Q signals from the digital section to produce a 102.4-μs chirp signal having a center frequency of 250 MHz and a 0.5 dB bandwidth of 80 MHz.

The signal switch unit (SSU) gates and distributes RF signals within the altimeter. It gates the 13.6-GHz signal from the UCFM and sends it to the Ku-band transmitter; it also gates the 13.1 GHz LO signal and sends it to the Ku-band MTU for the first down conversion process. It sends ungated 13.6 GHz, 13.1 GHz, and 500 MHz signals to the down converter unit (DCU) for conversion to C-band frequencies. The SSU also receives a 4.8 GHz chirped signal back from the DCU, gates it, and forwards it to the CMTU as the LO signal for the first C-band down conversion.

The DCU converts the two existing Ku-band signals, 13.6

Table 3 RF and Digital Units of the NRA

RF Units	Digital Units
1. Up Converter/Frequency Multiplier	1. Digital Signal Processor
2. Chirp Generator	a. Digital Filter Bank
3. Signal Switch Unit	b. Adaptive Tracker Assembly
4. Down Converter Unit	c. Synchronizer Assembly
5. Ku-band Amplifier (TWTA)	d. Interface Control Assembly
6. C-band Amplifier (CSSA)	2. Digital Portion, Chirp Generator
7. Microwave Transmission Units	
a. Ku-band	
b. C-band	
8. Receiver Unit	

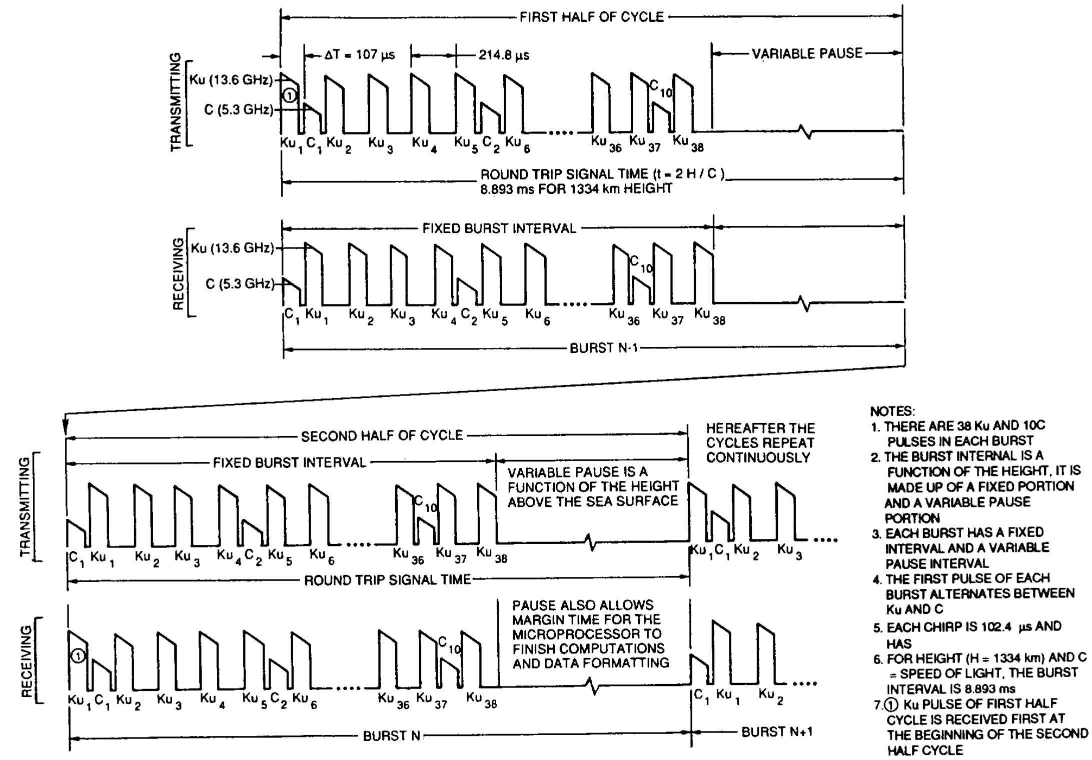

Fig. 9. The transmitted burst mode has interleaved Ku and C signals arranged so they are compatible for transmit and receive modes without interference.

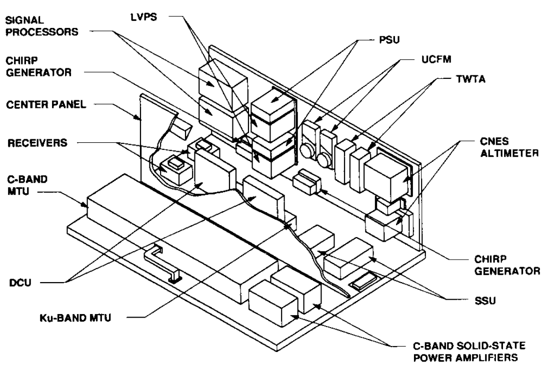

Fig. 10. The altimeter subsystem components are mounted in the F-section of the instrument module structure.

and 13.1 GHz, to C-band signals centered at 5.3 GHz and 5.1 GHz. As inputs the DCU uses the 13.1-GHz, 13.6-GHz, and 500-MHz signals produced in the UCFM and the stable 5-MHz reference provided by the spacecraft. Multiplication and coherent mixing in the DCU produces a 5.3-GHz chirped signal with a bandwidth (nominally) of 320 MHz for C-band transmission, and a 4.8-MHz chirped signal with the same bandwidth to be used as the LO signal for the first C-band downconversion in the receive chain.

The Ku-band transmitter is a traveling wave tube amplifier (TWTA). The traveling wave tube is very similar to the transmitter tube used on the Geosat altimeter. The electronic power conditioner (EPC) portion was redesigned to suit the needs of TOPEX/POSEIDON (higher PRF, etc.). The TWTA is powered directly from the spacecraft 28-V power bus through a relay in the power switching unit, and draws approximately 70 W of dc power during the normal range-tracking operation. The TWTA receives a 13.6-GHz gated chirp 102.4-μs signal from the SSU at a PRF of approximately 4200 pps. The level of this input is +5 dBm nominal. The TWTA amplifies this signal to a minimum level of 22 W and sends it to the Ku-band MTU (KMTU). The output will be a 22.4 W, 102.4 μs pulse linearly frequency modulated with a nominal bandwidth of 320 MHz. The pulse out of the TWTA should have a phase deviation across the pulse of no more than 4 degrees peak to peak and an amplitude variation of no more than 0.25 dB peak to peak. The TWTA incorporates internal protection for bus undervoltage, helix overcurrent, and converter overcurrent. It also has internal timing circuitry to prevent improper application of power.

The KMTU was designed, fabricated, and tested by APL. The KMTU is not redundant; however, all active components within the KMTU are redundant. It does take inputs from both TWTA's and operates with either receiver unit.

The C-band solid-state amplifier (CSSA) is the final

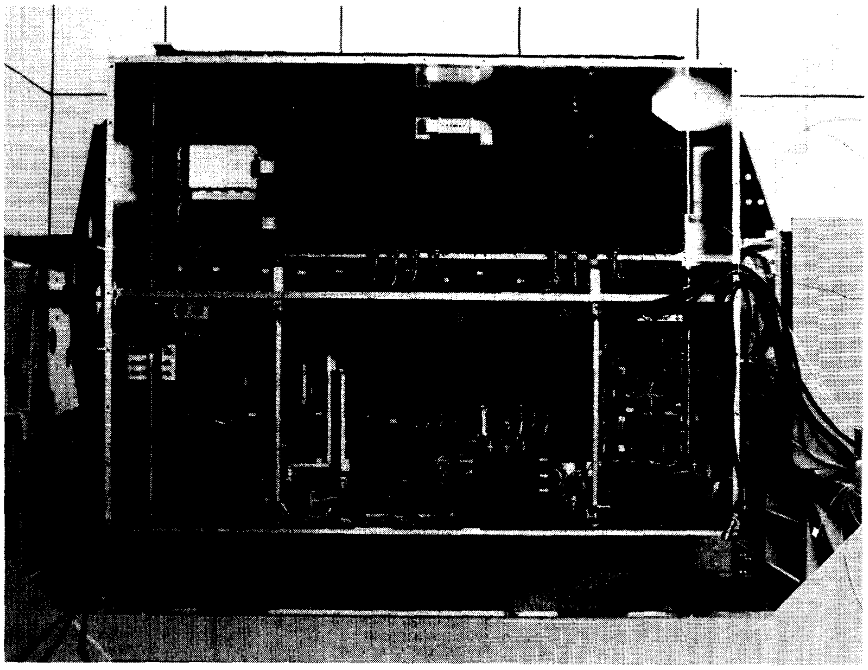

Fig. 11. This photograph presents the altimeter electronics flight units and harness arrangement internally within the instrument module nadir section.

transmitter amplifier for the other channel. The CSSA receives a 5.3-GHz chirped input signal from the DCU, amplifies it up to 20 W (43 dBm), and sends it to the CMTU. The input to the amplifier is nominally a 107.4-μs pulse with a center frequency of 5.3 GHz and a chirp bandwidth of 320 MHz. Its peak power level is approximately 0 dBm and its nominal PRF is 1220 pps. The CSSA is internally gated to produce a 102.4-μs output pulse. The amplifier can also be gated to provide a 33-μs output pulse with a bandwidth of approximately 100 MHz (narrow-band operation). The amplitude variation and phase ripple across the output pulse are to be no more than $\pm$ 0.25 dB and 6 degrees, respectively. The amplifier incorporates self-protection for higher input PRF or wider input pulses than desired. It also provides current limiting protection.

The amplifier portion of the CSSA comprises a driver amplifier and a high-power amplifier section. The driver amplifier has low- and medium-power sections. These sections provide limiting, temperature compensation, pulse shaping, and signal amplification. The high-power section provides two discrete stages of amplification and power combining. The CSSA also has a gating/telemetry section and a dc-to-dc converter for input power. The CSSA receives 28 V power directly from the spacecraft through relays in the power switching unit. The amplifying devices in the CSSA are all gallium arsenide field effect transistors. The CSSA was a completely new development designed specifically for the TOPEX/POSEIDON Project. The CSSA is described in more detail in [25].

Functionally, the C-band MTU (CMTU) is identical to the KMTU except that it operates with the C-band signal only. Since the NRA is the first altimeter to employ a C-band frequency, it is of a new design. The CMTU was designed, fabricated, and tested at the APL. An engineering model of this unit was fabricated and tested during the preproject Advanced Technology Model effort. This helped considerably in the flight model effort. All active components within the CMTU are redundant.

The CMTU receives transmission signals from the C-band solid-state amplifier and directs them either to the antenna for transmission or to the receiver via the calibrate path for internal self-calibration. In normal operation it directs the received signal from the antenna to the receiver. In the CMTU the transmission signal is monitored for peak power level and directed to the antenna through ferrite switching. Upon reception, the signal is preamplified (at RF), mixed in the first LO to IF (intermediate frequency = 500 MHz), filtered, and further amplified before being directed to the receiver. It also employs calibration circuitry that directs the transmission signal thru a precision calibration attenuator to the receive side of the CMTU for internal self-calibration.

The receiver alternately receives returned signals from each MTU in the dual frequency mode of operation. The signals passed from the MTU are both already converted to an intermediate frequency of 500 MHz before they are input to the receiver. The internal timing of the altimeter keeps track of whether the signals are from the C-band

Table 4 NRA Subassemblies Mass, Power, and Envelope Dimensions

Subassembly	Quantity	Mass (kg)	Power (W)	Dimensions (cm) W, L, H
Ku-band MTU	1	16.4	12.3	23 × 89 × 14
TWTA	2	11.2	70.0	37 × 25 × 8
Receiver (RCVR)	2	6.1	2.5	14 × 20 × 14
Upconverter (UCFM)	2	5.8	20.0	13 × 28 × 8
RF Chirp Generator	2	0.8	2.8	37 × 42 × 10
Digital Chirp Generator	2	2.2	9.0	10 × 16 × 9
Signal Switch Unit	2	7.4	2.8	29 × 17 × 10
Waveguide Assembly	Ku	0.5	N/A	N/A
C-band MTU	1	39.5	6.2	41 × 152 × 20
Solid-State Amplifier	2	10.1	28.0	17 × 25 × 13
Down Converter	2	20.7	16.4	14 × 27 × 9
Waveguide Assembly	C	4.0	N/A	N/A
Signal Processor	2	19.6	37.4	22 × 38 × 17
Low Voltage Power Supply	2	15.7	30.8	25 × 20 × 25
Power Switching	2	5.6	0.1	included with LVPS
Antenna and Feedhorn	1	15.2	N/A	1.5-m dish
Boresight Deck and Supports	1	6.9	N/A	N/A
Mounting Hardware	All	25.3	N/A	N/A
Thermal Blankets	All	4.0	N/A	N/A
French Waveguide	CNES	2.0	N/A	N/A
TOTALS	N/A	219 kg	238.3 W	N/A

channel or from the Ku-band. The receiver consists of two functional sections, the AGC section and the I/Q (inphase and quadrature) video section. The AGC section uses input signals from the digital processing section which are proportional to input power levels to set a digitally controlled attenuator. This is designed to keep the input signals to the digital signal processor at a constant level which is in the linear region of its operation. The repeatability of the attenuation at its setting is ±0.05 dB. During normal operation data from the AGC circuitry is used to determine a normalized return cross section which is relatable to surface wind speed. The I/Q video section down converts the IF signal to baseband quadrature video signals. These signals are amplified, filtered, and passed to the digital.

A summary of the subassemblies and their associated quantity, mass, power, and dimensions are shown in Table 4.

The digital section consists of the digital filter bank (DFB), adaptive tracker unit (ATU), synchronizer (SYNC), and the interface control unit (ICU). Figure 12 presents a functional schematic of the interconnecting relationships of these units. Basically, the signal processor converts the I and Q video signals to waveform samples which are processed within the ATU to produce the range and waveheight measurements.

The DFB performs the function of a power spectrum analyzer. The receiver video output is digitized during the receive gate windows which are 102.4 μs to produce 128 samples of each waveform. The transformation from the time domain to power spectral data is performed for both

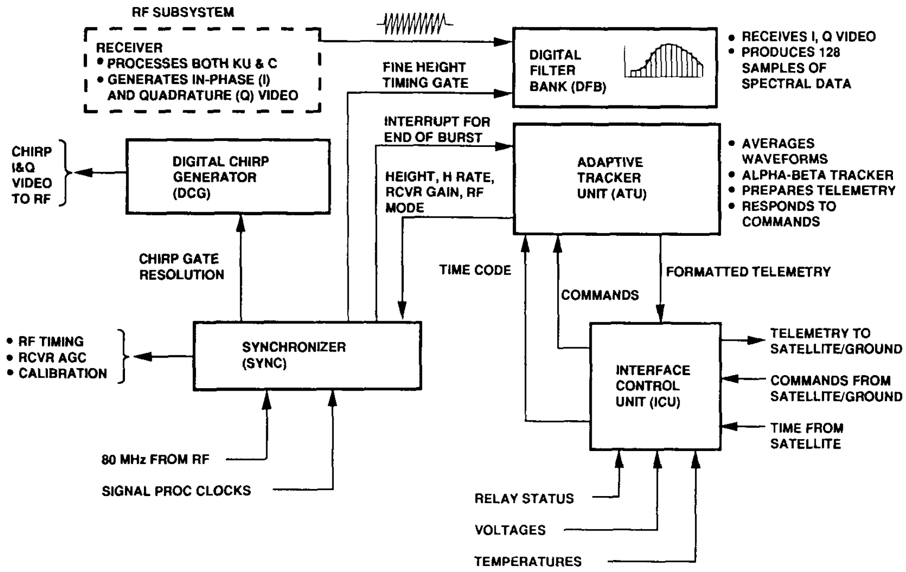

Fig. 12. The all digital signal processor converts I and Q video signals from the receiver into digitized waveforms, computes the height measurement, generates the telemetry output, and processes altimeter commands.

Ku- and C-band radars. The average power spectral data is then provided to the tracker unit.

The ATU uses an Intel 80186 microprocessor which runs the software that controls the altimeter. The second order alpha-beta algorithm is designed to track on the half-power point of the waveform. The resulting coarse and fine height information is shared with the synchronizer and the DFB to form a closed loop tracking system. The critical height and timing data are updated every six burst intervals which is about 50 ms. Subsequently, the ATU builds a frame of altimeter data every 20 update intervals or about once per second as a function of the altitude. Each altimeter record contains 20 height, waveheight, and AGC measurements averaged over the six burst intervals. Waveform samples are sent at the rate of 10 primary channel (normally Ku) and 5 secondary channel (normally C, however, they can be reversed upon proper commanding). The resulting data rate sent to the interface unit is slightly less than 10 kb/s.

The SYNC provides all clock and timing signals to the RF section, the DFB, and the ICU. The updated burst timing and gain control are provided to the RF unit for each transmit/receive interval.

The ICU interfaces the altimeter to the satellite bus. All telemetry and command functions are accomplished and metered through this unit. The telemetry data from the ATU are buffered and transferred to the satellite in a manner resulting in complete records of altimeter data. Due to the asynchronous altimeter telemetry the satellite bus oversamples in order to avoid losing data at lower altitudes when the altimeter data rate is highest.

The 1.5-m parabolic antenna directs the pencil-like radar beam to the ocean surface and receives the pulse-limited reflected signal. The antenna gain is 43.9 dB and the beamwidth is about 1.1 degrees for Ku and 2.7 degrees for C-band. The multifrequency feed horn accommodates both Ku- and C-band. The three radars are passively tied to the feed through on orthomode coupler that connects the NASA and CNES Ku-bands in quadrature with 30 dB of isolation. The antenna is honeycomb aluminum which is bonded to a mounting deck that holds the antenna securely and mounts to the satellite at 4 places. Figure 13 shows an end view of the antenna and F-section of the nadir portion of the instrument module.

A. Problems Overcome

1) The radiation environment posed a new challenge for altimeter radiation sensitive parts. At an altitude of 1334 ± 60 km the high energy protons and electrons are more severe than conventional altitudes of 830 ± 50 km. The Intel 80186 was subjected to a radiation test program. Ray tracing analysis was performed to characterize the environment at the part location. A total dose requirement of 72 krad over a 3 year period was established The total dose value included a design margin of two. Parts which exhibited a history of failure or permanent latchup due to single-event-upsets were disallowed. Decision was then made to appropriately spot shield the microprocessor and other radiation sensitive parts.

2) The C-band solid-state amplifier and RF chain was a new development. A preproject advanced technology mode (ATM) engineering unit was developed to prove-out the design. Additionally, the dual channel concept and return sig-

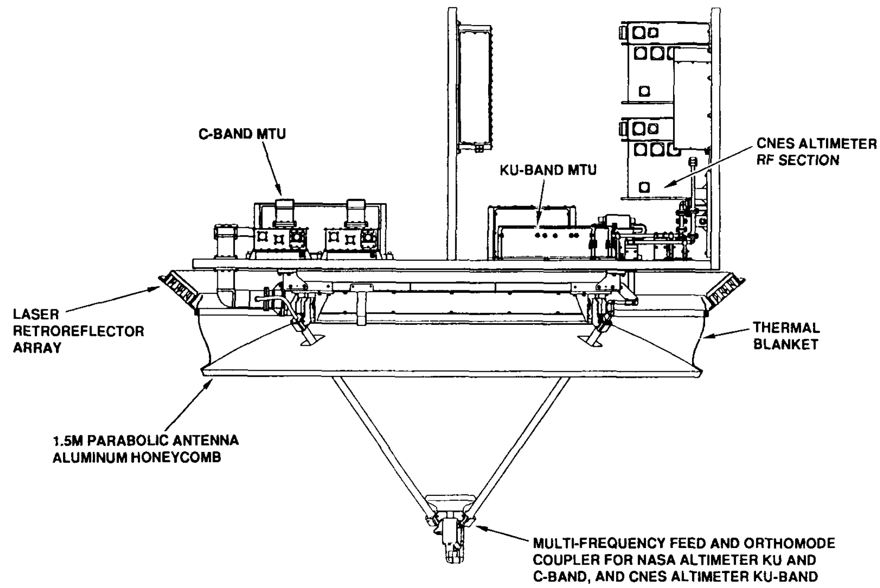

Fig. 13. An end view of the F-Section electronics and the 1.5-m antenna illustrates the configuration of the nadir portion of the instrument module.

nal simulator designs were developed to give confidence in the two frequency and high PRF design concept. The ATM reduced the risks for the NRA flight development program.

B. Prelaunch Testing

Each of the NRA subassemblies underwent functional test and checkout. The units were subjected to full environmental testing consisting of dynamic/vibration and thermal/vacuum tests. After integration of the subassemblies into the F-section, thermal/vacuum and EMI/EMC environmental tests were performed on the NRA at the GSFC facilities. Thermal/vacuum consisted of cycling between cold and hot limits, and hot soak. Each side of the redundant altimeter underwent approximately 168 hours of thermal/vacuum testing at GSFC. The assembled NRA will undergo sine vibration and acoustic tests as part of the satellite system tests. It was not meaningful to perform dynamic tests on the F-section alone. Considerable additional time on the NRA will be achieved during ambient system tests and during the long duration (45 day) thermal/vacuum test with the full-up satellite at the GSFC environmental test facility. The goal is to have at least 2000 hours on the flight hardware prior to launch. The height bias was measured several times during system test periods. Post launch, the height bias will be estimated during the verification phase.

C. Altimeter Operation

The NRA turn ON and operation will begin about fourteen days after launch. This will allow a sufficient period for outgassing to avoid any possibilities of arcing during high power TWTA operation. Once the NRA is initialized with any required software table updates, it will be placed in the normal track mode. This mode of operation is automatic, since the altimeter will track continuously over the ocean and also over land whenever the terrain is flat. The tracker logic will select the appropriate tracking parameters as the seastate varies. Whenever the altimeter loses lock, for instance, when the beam encounters uneven terrain over land, the tracker logic automatically reverts to the acquisition sequence until lock-up occurs. An onboard NRA internal calibration sequence will be performed twice each day to monitor any altimeter drift or change in performance.

When the CNES Radar Altimeter is ON, the NRA will be placed in the IDLE MODE. This configuration turns OFF the high power RF section and leaves the digital section ON. The amount of NRA power turned OFF is nearly equivalent to the CNES Altimeter. Then, the net power consumed does not imbalance the other subsystem's operating temperatures.

V. TOPEX Ground System Data Processing

The TOPEX Ground System (TGS) is being developed at the Jet Propulsion Laboratory (JPL). (See Fig. 14.) The TGS consists of software and hardware to generate commands, process telemetry, produce science and data products and to verify data. In each of these areas there has been significant interaction with the altimeter development team at WFF and the Science Working Team (SWT).

The standard data products are the Sensor Data Record (SDR) and the Geophysical Data Record (GDR). WFF developed most of the altimeter data correction algorithms. JPL developed most of the geophysical and control algorithms. Following development, the algorithms used to pro-

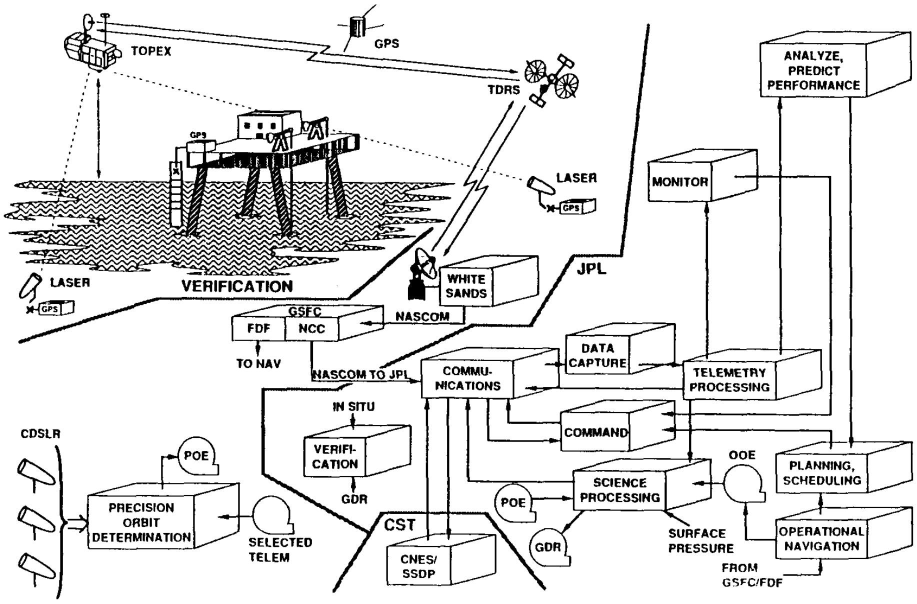

Fig. 14. The TOPEX ground system (TGS) functional diagram shows the downlink and uplink data flow and the primary elements of the system.

duce these products were reviewed in a series of algorithm walkthroughs conducted with the algorithm subcommittee of the SWT. These algorithms have been published [26].

The major verification will be performed at a point site located at an instrumented oil platform. The platform is an excellent site because of its low signal reflectivity and no signal contamination from land sources. Again, to ensure all aspects were understood, a number of workshops were held where the teams interacted for planning the verification. Those involved in workshop efforts included: ground system development (primarily JPL); altimeter instrument development (primarily WFF); and science data users (primarily Science Working Team). Interfaces to the Ground Data System are being defined by [27] and [28]. The interactions described above entailed much work, and it is believed that the end result will be valid, well understood altimeter data.

A. Verification Phase Assessment

A very intensive engineering assessment and verification period will commence with altimeter turn ON (about launch plus two weeks) and continue to the end of month six. During this phase, calibration data and selected altimeter science and engineering frames will be analyzed and evaluated daily. Additionally, a daily altimeter sensor performance summary will be monitored to detect any trends or abnormalities. This extended analysis will allow a more in-depth assessment of the altimeter data over a more extensive range of conditions. In-situ data from the verification site will be compared with altimeter measurements. In particular, the altimeter height will be compared with the laser ranging height for an absolute comparison. This will determine the in-flight height bias.

B. Observational Phase Assessment

The engineering assessment activities during the Observation Phase are less intense and will focus on altimeter performance in the following areas: height measurement noise, height measurement drift rate, AGC measurement noise, waveheight measurement noise, and acquisition time. In the interest of timeliness, significant findings will be reported informally as they occur. Calibration mode data will be monitored continuously. Altimeter drift, if any, and engineering performance summaries will be provided routinely by mission operations. Also, altimeter performance will be reported to the full science community at each SWT workshop.

C. Observational Phase Data Production

The primary data product for oceanographic research is the GDR which includes the altimeter height measurements, associated corrections, and measurement footprint locations based on the precision orbit ephemeris. The GDR will be generated on a global basis as an archival product. The GDR is provided to the science investigators who are members of the TOPEX/POSEIDON Project and will be available to the world science community. Science investigations, such as determination of the general circulation of the ocean and its variability; tests of the ability to compute circulation from the forcing by winds; descriptions of the nature of ocean dynamics, calculation of the transport of heat, mass, nutrients, and salt by the oceans; the determination of geocentric tides; and the investigation of ocean currents with waves, are among the principal investigations that will be performed by the science community.

VI. Summary

In summary, the TOPEX/POSEIDON Project NRA will be the premier scientific instrument of the 1990's for ocean topography. Based on heritage technology from Seasat and Geosat, the NRA is the next extension in a high technology and conservative design altimeter. The NRA, with two frequencies to account for the ionospheric path delay and fully redundant to provide for high reliability and long life, is expected to fulfill all its objectives. Project timing, astutely programmed by NASA and CNES, compliments the World Ocean Circulation Experiment (WOCE), the Tropical Oceans Global Atmospheres (TOGA), the European Space Agency ESA-1 satellite, and during the probable extended mission, the NASA Scatterometer (NSCAT) program, currently planned for launch on a Japanese satellite. Naturally, we have high expectations for the successful testing, launch in 1992, and subsequent operation of the NRA. The TOPEX/POSEIDON Project will acquire a dedicated set of altimetry data on ocean topography that will provide years of data for oceanographers.

Acknowledgment

The authors wish to recognize the contributions to this task by L. C. Rossi, GSFC NRA Manager; F. J. Logan, JHU/APL NRA Manager; and J. L. MacArthur, JHU/APL NRA Scientist. They also wish to thank the rest of the team members involved in the NRA development, particularly, the engineers and fabrication personnel at JHU/APL, and the support group at GSFC.

References

[1] *Seasat Special Issue I: Geophysical Evaluation, J. Geophys. Res.*, vol. 87, no. C5, pp. 3173–3438, Apr. 1982.
[2] *Seasat Special Issue II: Scientific Results, J. Geophys. Res.*, vol. 88, no. C3, pp. 1529–1952, Feb. 1983.
[3] *Geosat Special Issue Part 1, J. Geophys. Res.*, vol. 95, no. C3, Mar. 1990.
[4] *Geosat Special Issue Part 2, J. Geophys. Res.*, vol. 95, no. C10, Oct. 1990.
[5] "Requirements and constraints for the NASA Radar Altimeter," Document 633–420 (internal document), Jet Propulsion Laboratory, Pasadena, CA, 1989.
[6] G. S. Brown, H. R. Stanley, and N. A. Roy, "The wind speed measurement capability of spaceborne radar altimeters," *IEEE J. Oceanic Eng.*, vol. OE-6, pp. 59–63, 1981.
[7] D. B. Chelton, and P. J. McCabe, "A review of satellite altimeter measurement of sea surface wind speed: With a proposed new algorithm," *J. Geophys. Res.*, vol. 90, pp. 4707–4720, 1985.
[8] J. T. McGoogan, L. S. Miller, G. S. Brown, and G. S. Hayne, "The S-193 radar altimeter experiment," *Proc. IEEE*, vol. 62, pp. 793–803, June 1974.
[9] H. R. Stanley, "The Geos-3 project," *J. Geophys. Res.* vol. 84, no. B8, pp. 3779–3783, July 1979.
[10] J. L. MacArthur, "Design of the SEASAT-A radar altimeter," in *Proc. Oceans '76*, Washington, DC, September 13–15, 1976, (New York: Marine Technology Society and IEEE), pp. 10B-1–10B-8.
[11] J. L. MacArthur, "Seasat-A radar altimeter design description," *Doc. SDO-5232*, Applied Physics Laboratory, Johns Hopkins University, Laurel, MD, Nov. 1978.
[12] J. L. MacArthur, P. C. Marth, and J. G. Wall, "The GEOSAT radar altimeter," *Johns Hopkins APL Tech. Digest*, vol. 8, no. 2, pp. 176–181, Apr. 1987.
[13] J. L. MacArthur and P. V. K. Brown, "Altimeter for the ocean topography experiment (TOPEX)," *SPIE—Recent Advances in Civil Space Remote Sensing, Society of Photo-Optical Instrumentation Engineers*, vol. 481, Bellingham, WA, 1984.
[14] "TOPEX altimeter system specification," Document 7301–9028, Applied Physics Laboratory, Johns Hopkins University, Laurel, MD, Oct. 1990.
[15] J. L. MacArthur, C. C. Kilgus, C. A. Twigg, and P. V. K. Brown, "Evolution of the satellite radar altimeter," *Johns Hopkins APL Tech. Digest*, vol. 10, no. 4, pp. 405–413, Oct. 1989.
[16] *Geos 3 Special Issue, J. Geophys. Res.* vol. 84, no. B8, pp. 3779–4079, July 1979.
[17] *Theme Issue: Satellite Altimetry, Marine Geodesy*, vol. 8, no. 1–4, 1984.
[18] D. B. Chelton, E. J. Walsh, and J. L. MacArthur, "Pulse compression and sea level tracking in satellite altimetry," *J. Atmospheric and Oceanic Technol.*, vol. 6, no. 3, pp. 407–438, June 1989.
[19] R. K. Moore and C. S. Williams, Jr., "Radar terrain return at near-vertical incidence," *Proc. IRE*, vol. 45, no. 2, pp. 228–238, Feb. 1957.
[20] G. S. Brown, "The average impulse response of a rough surface and its applications," *IEEE Trans. Antennas Propagat.*, vol. AP-25, pp. 67–74, Jan. 1977.
[21] Rodriguez, E., "Altimetry for non-Gaussian oceans: Height biases and estimation of parameters," *J. Geophys. Res.*, vol. 93, no. C11, pp. 14 107–14 120, 1988.
[22] E. Rodriguez and B. Chapman, "Extracting ocean surface information from altimeter returns: The deconvolution method," *J. Geophys. Res.*, vol. 94, no. C7, pp. 9761–9778, 1989.
[23] B. J. Lipa and D. E. Barrick, "Ocean surface height-slope probability density function from SEASAT altimeter echo," *J. Geophys. Res.*, vol. 86, pp. 10 921–10 930, 1981.
[24] J. Goldhirsh and J. R. Rowland, "A tutorial assessment of atmospheric height uncertainties for high precision satellite altimeter missions to monitor ocean currents," *IEEE Trans. Geosci. Remote Sensing*, vol. GE-20, no. 4, pp. 418–434, Oct. 1982.
[25] U. I. Von Mehlem and R. E. Wallis, "Solid-state power amplifiers for satellite radar altimeters," *Johns Hopkins APL Tech. Digest* vol. 10, no. 4, pp. 414–422, Oct. 1989.
[26] P. S. Callahan, Ed., "TOPEX ground system science algorithm specification," Document 633–708 (internal document), Rev. A, Jet Propulsion Laboratory, Pasadena, CA, Sept. 1990.
[27] "Software interface specifications, TOPEX/POSEIDON project," Document 633–731 (internal document), Jet Propulsion Laboratory, Pasadena, CA, 1990.
[28] "Interface control document to GSFC/WFF, TOPEX/POSEIDON project," Document 633–712J (internal document), Jet Propulsion Laboratory, Pasadena, CA, 1990.

Alfred R. Zieger was born in Austin, TX, on July 6, 1940. He received the B.S. degree in aerospace engineering at the University of Texas at Austin in 1965.

He initially joined the Boeing Company and worked on the Lunar Orbiter, Apollo, and Mariner Venus-Mercury Projects. He joined the Jet Propulsion Laboratory in 1977 while working on the Voyager Project. While on Voyager, he was the Spacecraft Team Chief Deputy, the Mission Control Team Chief, and the Operations Coordination Team Chief. In 1983 he became part of the TOPEX/POSEIDON Project where he served as the Sensors System Manager. He is presently Mission Manager of the TOPEX/POSEIDON Project.

Mr. Zieger is a member of AIAA ('64) and a recipient of the NASA Exceptional Service Medal.

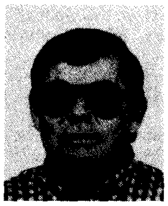

Craig L. Purdy was born in Chincoteague, VA, on June 2, 1947. He received the B.S. degree in electrical engineering from Virginia Polytechnic Institute in 1970.

Since 1970 he has been with the National Aeronautics and Space Administration at the Goddard Spaceflight Center, Wallops Flight Facility, in Wallops Island, VA, in the Radar and Optical Systems Section. He was a system engineer on the SKYLAB S-193 Radar Altimeter, the Experiment Manager on the GEOS-3 Radar Altimeter, the Systems Engineer on the SEASAT Radar Altimeter, and is presently the Sensor Development Manager for the TOPEX/NASA Radar Altimeter.

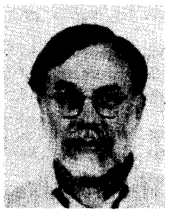

George S. Hayne (Member, IEEE) was born in 1937 in Ann Arbor MI. He received the B.A. degree in physics in 1958 from Kalamazoo College, Kalamazoo, MI, and the Ph.D. degree in physics in 1966 from Yale University, New Haven, CT. He did post-doctoral work in physics at Duke University, Durham, NC.

He held staff positions at the Research Triangle Institute, Research Triangle Park, NC, and at Applied Science Associates, Apex, NC. Since 1980, he has been with the NASA Goddard Space Flight Center's Wallops Flight Facility at Wallops Island, VA. His current technical interests are in the general area of remote sensing of planetary surfaces, and the specific areas of radar altimetry and its associated data correction and processing.

Dr. Hayne is a member of the American Geophysical Union and of Sigma Xi.

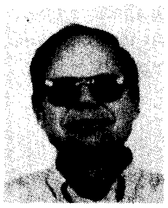

David W. Hancock was born in Stockton, MD, in 1946. He received the B.S. degree in mathematics from East Carolina University, Greenville, NC in 1970.

In 1964, he joined NASA Wallops Flight Center, Wallops Island, VA, as an electronic technician apprentice and completed its requirements in 1968. From 1970 to present he has been at the NASA Goddard Space Flight Center's Wallops Flight Facility. He has worked on the real-time computer control for radar and laser altimeters and algorithms for ground processing of the altimeter data. He is presently a Sensor Scientist for the TOPEX/NASA Radar Altimeter.